VERSITA

Cent. Eur. J. Chem. • 12(2) • 2014 • 220-226
DOI: 10.2478/s11532-013-0366-5

Central European Journal of **Chemistry**

The synthesis, structure and physical properties of lanthanide(III) complexes with nicotinic acid

Research Article

Nuša Hojnik[1*], Matjaž Kristl[1], Amalija Golobič[2], Zvonko Jagličić[3], Miha Drofenik[1,4]

[1]*University of Maribor, Faculty of Chemistry and Chemical Engineering, SI-2000 Maribor, Slovenia*

[2]*University of Ljubljana, Faculty of Chemistry and Chemical Technology, SI-1000 Ljubljana, Slovenia*

[3]*Institute of Mathematic, Physics and Mechanics, 1000 Ljubljana, Slovenia and Faculty of Civil and Geodetic Engineering, 1000 Ljubljana, Slovenia*

[4]*Jožef Stefan Institute, SI-1000 Ljubljana, Slovenia*

Received 12 July 2013; Accepted 7 October 2013

Abstract: This article reports the synthesis of novel, rare-earth coordination complexes with nicotinic acid. Three compounds with the general formula $Ln_2[(C_5H_4NCOO)_6(H_2O)_4]$ (Ln = Yb, **1**; Ln = Gd, **2**; Ln = Nd, **3**) were prepared from relatively cheap and readily available reactants. Their compositions and structure were characterized by IR spectroscopy and single-crystal X-ray diffraction. The magnetic and thermogravimetric properties were also studied. The complexes consist of centrosymetric, dimeric molecules having all six nicotinato ligands coordinated with the central atom in the bidentate mode. The coordination environment of the Ln^{3+} for all three compounds is 8. Here we describe the crystal structure of Yb and Gd complexes with nicotinic acid.

Keywords: *Lanthanides • Nicotinic acid • Magnetic properties • X-ray structure determination • Hydrogen bonds*

1. Introduction

The complexes of pyridine carboxylic acids, namely nicotinic, picolinic and isonicotinic acids, have been the subject of several investigations in the past decade. In this investigation we have looked at complexes that contain nicotinic acid (NIC) because of its coordination mode. Besides the structural studies of these complex compounds, in connection with the chemical systematics, these coordination compounds also exhibit useful properties, which has led to their use in various fields, including electronics, for instance in electroluminescent devices [1], in analytical tools [2], in functional biological assays [3,4] and in medical imaging devices [5]. To date, a series of $[Ln_2(NIC)_6(H_2O)_4]$ complexes have been reported with Ln = Eu(III), Tb(III), Nd(III) and some others (for Nd(III) this is a record in a database from 1996) [6-9]. Here we report on the synthesis of new compounds of the type $[Yb_2(NIC)_6(H_2O)_4]$ **1**, $[Gd_2(NIC)_6(H_2O)_4]$ **2**, $[Nd_2(NIC)_6(H_2O)_4]$ **3**, their crystal structures and physical properties.

The ligand nicotinic acid can be described as an unsymmetrical divergent ligand with a nitrogen atom at one end and two carboxylate oxygen atoms at the other end. Nicotinate anions are useful unities in forming an extended structure [10-12]. Here, the carboxylate groups and the pyridine function as soft bases, while the rare-earth metals are hard acids (Lewis acid). For this reason the rare-earth metals are coordinated with the carboxylate part of the ligand and

* *E-mail: nusa.hojnik@um.si*

with the N donor of the pyridine ring, forming stable complexes [13]. It is known that the absorption ability of lanthanides for UV light is very weak [14,15], while their absorption coefficient can be increased in coordination compounds with organic ligands, such as *β*–diketonates, aromatic carboxylic acid and heterocyclic derivatives [16,17]. These organic ligands can absorb UV light and transfer the absorbed energy to lanthanide ions ("antenna effect").

2. Experimental procedure

2.1. Synthesis

All the reactants of A.R. grade were obtained commercially and used without further purifications.

$[Yb_2(NIC)_6(H_2O)_4]$ **1**

The nicotinic acid (0.123 g, 1.0 mmol) was completely dissolved in distilled water (10 mL). With the slow addition of solid sodium hydroxide (0.04 g, 1.0 mmol), a clear solution was formed, to which $Yb(NO_3)_3$•$5H_2O$ (0.225 g, 0.5 mmol) was added under stirring. The sample was put in a fridge and left there for 2 weeks. Colourless single crystals, suitable for analysis, were obtained, by slow evaporation of the solvent. Yield: 48%.

$[Gd_2(NIC)_6(H_2O)_4]$ **2**

This complex was prepared with the procedure described for **1** using $Gd(NO_3)_3$•$6H_2O$ (0.226 g, 0.5 mmol) and nicotinic acid (0.123 g, 1.0 mmol). Colourless single crystals, suitable for analysis, were obtained. Yield: 45%.

$[Nd_2(NIC)_6(H_2O)_4]$ **3**

This complex was prepared with the procedure described for **1** using $Nd(NO_3)_3$•$6H_2O$ (0.219 g, 0.5 mmol) and nicotinic acid (0.123 g, 1.0 mmol). Violet single crystals, suitable for analysis, were obtained. Yield: 45%.

2.2. Thermal analysis

A thermogravimetric analysis was carried out on a METTLER TGA/SDTA851^e system in the temperature range 30–1200°C in a nitrogen flow (100 mL min^{-1}) with a heating rate of 10 K min^{-1} using Al_2O_3 crucibles.

2.3. XRPD analysis

X-ray powder diffraction data for the products of the thermal decomposition were collected with an AXS-Bruker/Siemens/D5005 diffractometer using CuK_a radiation at 293 K. Finely ground samples were placed on a Si single-crystal holder and measured in the range $10° < 2q < 70°$. The diffraction data was analysed using the EVA program and the PDF Datafile.

2.4. Magnetic measurements

The magnetic properties of the compounds were measured using a Quantum Design MPMS-XL-5 susceptometer equipped with a SQUID detector. The data were collected between 2 K and 300 K at a magnetic field of 0.1 T. The measured data are already corrected for the sample-holder contribution and for the temperature-independent Larmor diamagnetism of the core electrons obtained from Pascal's tables.

2.5. X-ray structure determination

The crystal data and refinement parameters of compounds **1** and **2** are listed in Table 1. Single-crystal diffraction data for both compounds were collected on a Agilent SuperNova dual-source diffractometer with an Atlas detector at room temperature with Mo Kα radiation (0.71073 Å). The data were processed using CrysAlis PRO software [18]. The structure was, in both cases, solved with direct methods using SIR97 [19]. A full-matrix, least-squares refinement on F2 was employed with anisotropic temperature displacement parameters for all the non-hydrogen atoms. The hydrogen atoms from the water molecules were located in a difference Fourier map; the remaining were placed at calculated positions and treated as riding, with C—H 0.93 Å and Uiso(H) = 1.2 Ueq(C). The parameters of the hydrogen atoms from the water molecules were not refined, with the exception of their isotropic displacement parameters in **1**. SHELXL97 software [20] was used for the structure refinement and interpretation. Drawings of the structures were produced using ORTEPIII [21] and Mercury [22]. The crystal structure of compound **3** was also determined as described above. Since the structure has already been published [8], no further structural details are given.

3. Results and discussion

3.1. Crystal and molecular structure

The structures of **1** and **2** consist of centrosymetric, dimeric molecules with the formula

$[Ln_2(\mu\text{-}OOCC_5H_4N)_4(OOCC_5H_4N)_2(H_2O)_4]$,

where Ln is Yb^{3+} and Gd^{3+}, respectively.

Ortep drawings of both complexes are shown (Figs. 1 and 2).

Compounds **1** and **2** are isostructural with the La, Pr, Nd, Sm, Eu, Tb, Dy, Ho, Er and Tm complexes [6-9]. All six nicotinato ligands are coordinated with the central atom in the bidentate mode *via* both oxygen atoms of

Table 1. Summary of crystallographic data and structure analyses.

Compound	1	2
Empirical formula	$[Yb_2(O_2C_6H_4N)_6(H_2O)_4]$	$[Gd_2(O_2C_6H_4N)_6(H_2O)_4]$
Relative molecular weight, M_r	1150.76	1119.18
Cell setting, space group	monoclinic, $P2_1/c$	monoclinic, $P2_1/c$
Temperature (K)	293(1)	293(1)
a (Å)	9.5065(2)	9.6277(3)
b (Å)	11.5408(3)	11.6911(4)
c (Å)	17.8513(4)	17.7098(6)
β (°)	91.092(2)	91.867(3)
V (Å^3)	1958.16(8)	1992.33(11)
Z	2	2
D_x (Mg m^{-3})	1.952	1.866
Radiation type, wavelength (Å)	Mo *K*α, 0.71073	Mo *K*α, 0.71073
μ (mm^{-1})	4.828	3.380
F(000)	1116	1092
Crystal form, colour	prism, colourless	prism, colourless
Crystal size (mm)	0.16 × 0.08 × 0.04	0.35 × 0.30 × 20
Absorption correction	multiscan	multiscan
No. of measured and indep. reflec.	13114, 5229	12855, 5221
No of (F^2>2.0σ(F^2)) reflections	4333	4090
R_{int}	0.036	0.050
Θ range (°)	2.9 – 27.5	2.7 – 27.5
Full-matrix refinement on	F^2	F^2
$R[F^2 > 2\sigma(F^2)]$, $wR(F^2)$, S	0.027, 0.051, 1.05	0.044, 0.124, 1.07
$\Delta\rho_{max}$, $\Delta\rho_{min}$ (eÅ^{-3})	0.81, -0.71	3.01, -1.15
No. of parameters	275	271
No. of contributing reflections	5229	5221

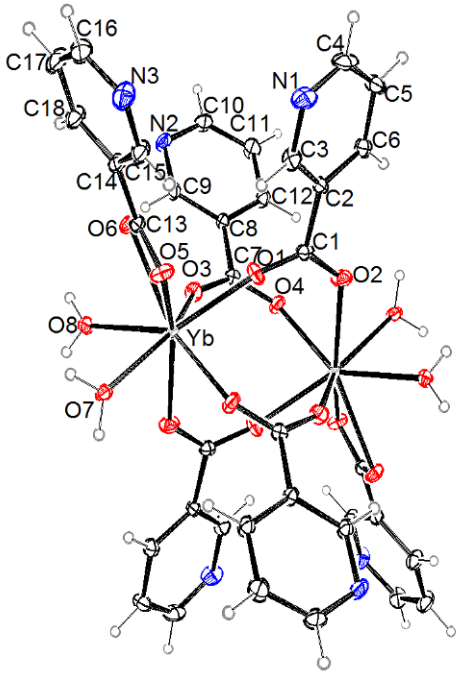

Figure 1. ORTEP drawing of coordination molecules of **1**. Ellipsoids are at 30% probability level. Labelled are non-H atoms from the asymmetric unit.

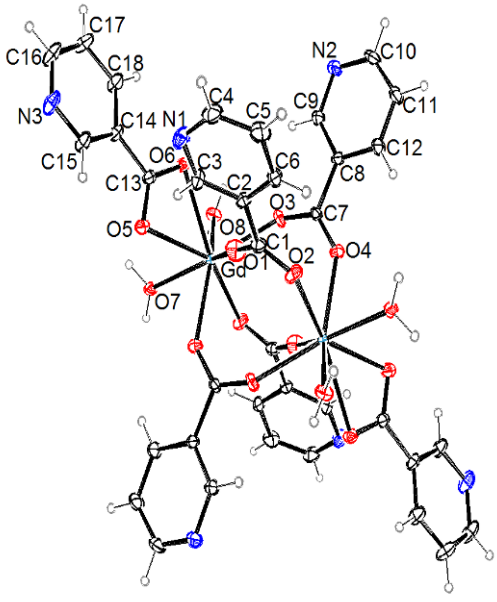

Figure 2. ORTEP drawing of coordination molecules of **2**. Ellipsoids are at 30% probability level. Labelled are non-H atoms from the asymmetric unit.

the carboxylate group. Four of them form four *syn-syn* bridges between both central atoms of the coordination molecule. The remaining two are bonded terminally as *syn-syn* chelates. The coordination sphere is completed with two water molecules bonded in the *cis* mode. In this way each central atom is coordinated with 8 oxygen atoms. The coordination polyhedron is a slightly distorted, bicapped, trigonal prism. Selected bond lengths for both compounds are given in Table 2. In both compounds the bridging Ln-O bonds are the shortest, *i.e.*, 2.258(2)–2.289(2) and 2.331(4)–2.374(4) Å for 1 and 2, respectively, and the Ln-O from the chelate is the longest, *i.e.*, 2.422(2), 2.456(2) and 2.473(3),

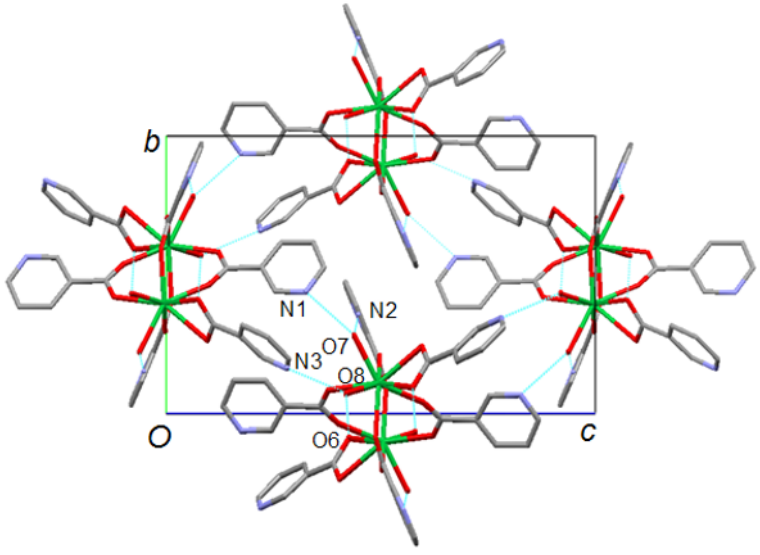

Figure 3. Mercury drawing of crystal packing of molecules in 1 viewed along the a axis. Hydrogen atoms are omitted for clarity. The light-blue lines represent the hydrogen bonds.

Table 2. Selected bond lengths in (Å) in **1** and **2**.

O1—Yb	2.258 (2)	O1—Gd	2.331 (4)
O2—Ybi	2.289 (2)	O2—Gdi	2.374 (4)
O3—Yb	2.269 (2)	O3—Gd	2.348 (4)
O4—Ybi	2.281 (2)	O4—Gdi	2.356 (3)
O5—Yb	2.456 (2)	O5—Gd	2.535 (4)
O6—Yb	2.422 (2)	O6—Gd	2.473 (3)
O7—Yb	2.327 (2)	O7—Gd	2.395 (4)
O8—Yb	2.342 (2)	O8—Gd	2.419 (3)

Symmetry code: i: 1-x, -y, 1-z

2.535(4) Å for **1** and **2**, respectively. The water molecules are bonded at distances of 2.327(2), 2.342(2) and 2.395(4), 2.419(3) Å for **1** and **2**, respectively. The Gd-O bond lengths are in all cases longer then the corresponding Yb-O ones due to the smaller ionic radius of the Yb^{3+} in comparison with the Gd^{3+}, *i.e.*, 0.985 and 1.053 Å, respectively [23]. The Gd-Gd distance within the dimer, *i.e.*, 4.3618(3) Å, is only slightly longer than the Yb-Yb distance, *i.e.*, 4.3538(2) Å.

The crystal packing of the molecules in **1** is shown (Fig. 3). The molecules of **2** are packed in the crystal in the same way. In both compounds the packing of the molecules is stabilised by intermolecular hydrogen bonds, the geometry of which is presented in Table 3. Each water molecule is a donor of two intermolecular hydrogen bonds through both their hydrogen atoms. The acceptors are N atoms of all the nicotinato ligands and the O6 atom from the chelate-carboxylate group. As already mentioned, the contraction of the cation radius is reflected in shorter coordination bond lengths in **1** in comparison with **2**, which has the consequence that the molecules of **1** have a smaller dimension than those of **2**. It is interesting that in spite of being smaller molecules only the *a* and *b* edges of the unit cell are smaller in **1,** while *c* is longer in comparison with those in **2**. The reason is that the intermolecular interactions along the *c* axis are weaker in **1** than in **2**, which can be concluded from the contact distances between the O and N atoms from the O7-H…N1 and O8-H…N3 hydrogen bonds, which are longer in **1** than in **2**. Selected bond lengths and bond angles formed by the metal atoms are listed in Tables 2 and 3. The water molecules are positioned so as to permit hydrogen bonding to the nitrogen atoms.

3.2. Thermogravimetric measurements

The TGA–DTG curves of the thermal decomposition process of $[Yb_2(NIC)_6(H_2O)_4]$ (Fig. 4) can be divided into three steps. The first initial drift on the curve can be attributed to the loss of adsorbed water. Under our experimental conditions, the compound is stable up to 110°C and undergoes three decomposition steps by heating to 1200°C. In the first step, between 110-230°C, there is a mass loss of 6.3%, which is in good agreement with the value calculated for the release of water from the coordination sphere (Δm_{calc} = 6.3%) In the second step, between 370 - 550°C, the sample loses 39.6% of its initial weight. This is the main process containing two partly-separated decomposition steps, which are related to the proposed reaction of the decomposition of carboxylate groups. Finally, there is a

Table 3. Geometrical parameters of intermolecular hydrogen bonds in **1** and **2**.

D—H···A	D···A (Å)	D—H (Å)	H···A (Å)	D—H···A(°)
O7-HW3…N1^{i}	1	0.858	2.102	146.76
	2	1.046	1.881	151.99
O7-HW4…N2^{ii}	1	0.868	1.893	172.92
	2	0.936	1.871	158.42
O8-HW2…N3^{i}	1	0.756	2.074	162.70
	2	0.977	1.819	158.71
O8-HW1…O6^{ii}	1	0.816	1.970	169.15
	2	0.734	2.072	160.43
O7-HW3…N1^{i}	1	0.858	2.102	146.76
	2	1.046	1.881	151.99
O7-HW4…N2^{ii}	1	0.868	1.893	172.92
	2	0.936	1.871	158.42

Symmetry codes: i: x,-y-1/2 z+1/2, ii: -x+2,-y,-z+1

mass loss above 550°C, which in the beginning is steep, but then becomes more gradual, which indicates the gradual decomposition of the nicotinato ligands. At the end, rare-earth oxides are the final products; these were characterized by X-ray powder diffraction. The total mass loss up to 1200°C (Δm_{meas} = 65.5%) agrees with the theoretical value calculated by taking Yb_2O_3 as the final product (Δm_{calc} = 65.7%). The TGA and DTG curves of the complexes **2** and **3** (Fig. 5) are similar to that of complex **1**. The total measured weight loss for both compounds is about 67.3% and 69%, which is in good agreement with the values calculated by taking Gd_2O_3 (Δm_{calc} = 67.5%) and Nd_2O_3 (Δm_{calc} = 69.2%) as the final product. Similar behaviour was reported for samarium complex with nicotinic acid [24].

3.3. IR assessments

The IR spectra of the compounds were recorded in the region from 4000 to 400 cm^{-1} on KBr pellets. They were then compared with each other as well as with ligand spectrum, which are shown in Table 4 [25]. The bands in the compounds **1**, **2**, **3** are in the range of ν_s(O–C–O) (1408–1477 cm^{-1}). However, there are some differences between the compounds in the positions of the respective bands in the nicotinic acid (1370–1488cm^{-1}).Suchashiftiscausedbythecoordination of the nicotinic to the Ln^{3+} ion through the oxygen atoms of the carboxyl groups. A similar dependence of ν_{as}(O–C–O) (1627–1654 cm^{-1}) frequencies is also noted for all the compounds. The value set of the $\nu_s(H_2O)$ vibration bands of a water molecule is in a range (3055–3097 cm^{-1}) and $\nu_{as}(H_2O)$ (3132–3317 cm^{-1}).

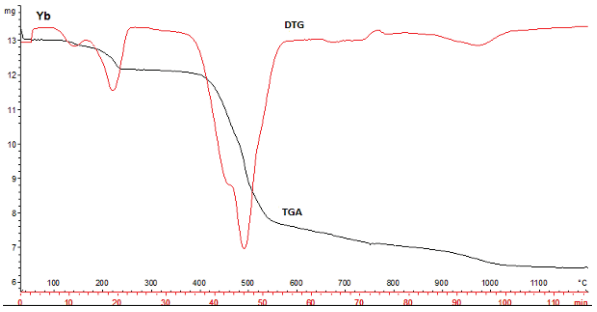

Figure 4. TGA-DTG curves showing the decomposition of $[Yb_2(NIC)_6(H_2O)_4]$ at a heating rate of 10 (K min^{-1}) in a nitrogen atmosphere.

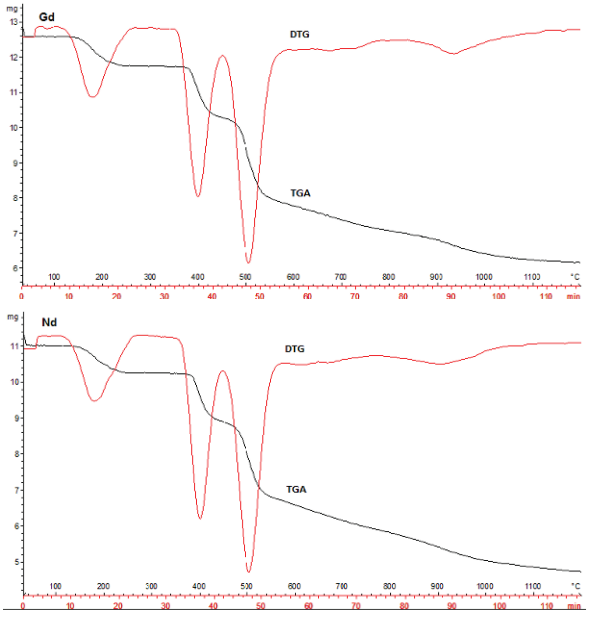

Figure 5. TGA-DTG curves showing the decomposition of $[Gd_2(NIC)_6(H_2O)_4]$ and $[Nd_2(NIC)_6(H_2O)_4]$ at a heating rate of 10 K min^{-1} in a nitrogen atmosphere.

The absence of the 1709 cm^{-1} band corresponding to ν(C=O) in the IR spectra of the compounds evidences the deprotonation of the carboxyl group [26]. The reason for this is that the nicotinic acid must be bridging-chelating bonded to the central lanthanide atom with the involvement of the oxygen atoms of the carboxyl groups, as in the structure described for the complex.

3.4. Magnetic properties

At high temperatures effective magnetic moment p_{eff} of all the compounds exhibits a constant value indicating paramagnetic behaviour. Susceptibility can be well described by the Curie-Weiss formula (Eq. 1),

$$\chi = \frac{C}{(T-\theta)} \quad (1)$$

Table 4. Values of some bands in the IR absorption spectrum of compounds, **1**, **2**, **3** and the ligand nicotinic acid (NIC).

1, cm^{-1}	2, cm^{-1}	3, cm^{-1}	NIC	Assignment
759(m)	759(m)	748(m)	748(m)	δ(C–H)
1408(s)	1408(s)	1431(s)	1415(s)	$\nu_s(COO^-)$
1550(m)	1546(m)	1543(m)	1489(m)	ν(C–C), ν(C–N)
1593(s)	1593(s)	1593(s)	1589(s)	ν(C–C), ν(C–N)
1654(s)	1643(s)	1627(s)	1708(s)	$\nu_{as}(COO^-)$
2364(m)	2364(m)	2364(m)	2364(m)	ν(N—H)
3059(m)	3055(m)	3062(m)	3071(m)	$\nu_s(H_2O)$
3097(m)	3093(m)	3089(m)	3104(w)	$\nu_s(H_2O)$
3255(m)	3178(m)	3317(m)	3447(m)	$\nu_{as}(H_2O)$

Table 5. Curie constants and effective magnetic moments of Ln(III).

Sample	Ln^{3+}	C (emu K mol^{-1})	μ_{eff} (BM)
1	Yb	2.92	4.8
2	Gd	7.66	7.8
3	Nd	1.79	3.8

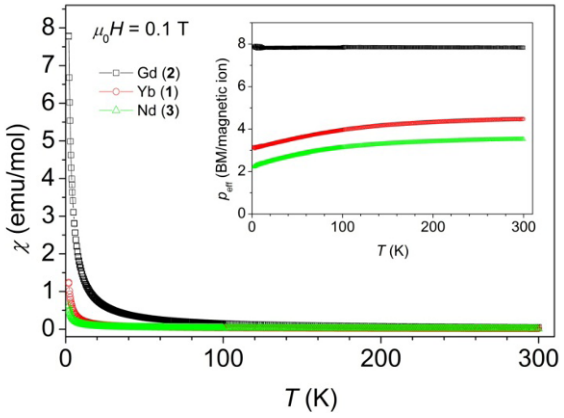

Figure 6. Molar susceptibility as a function of temperature measured in a magnetic field of 0.1 T. Inset shows an effective magnetic moment as a function of temperature calculated per magnetic ion.

where C is the Curie constant. For all compounds the measured C values and the corresponding magnetic moments in Table 5 agree satisfactorily with the expected spin-only moments for free Yb^{3+} (4.5 BM), Gd^{3+} (8 BM), and Nd^{3+} (3.5 BM) calculated with the Russell-Sandres (L-S) coupling scenario [27]. Slight decrease of the effective magnetic moment with decreasing temperature in the compounds **1** and **3** is due to the temperature dependent spin-orbit coupling (Fig. 6). For the sample **2** effective magnetic moment remains constant down to the lowest temperature since L=0 for $4f^7$ configuration of Gd^{3+} ions and there is no spin-orbit coupling [27].

4. Conclusions

In conclusion, three water-soluble coordination compounds of lanthanides and nicotinic acid with the general formula $Ln_2[(C_5H_4NCOO)_6(H_2O)_4]$ have been prepared. The thermal decomposition of all compounds was studied by thermogravimetric analysis and X-ray powder diffraction, yielding lanthanide oxides as final products. Magnetic properties can be explained by the strong coordination of carboxylate group to the Ln(III) acceptor and the and high paramagnetic character of rare earth ions. Finally, the crystal structure of the novel Yb and Gd compounds has been determined by single-crystal X-ray analysis, revealing a structure consisting of dimeric $Ln_2[(C_5H_4NCOO)_6(H_2O)_4]$ molecules, packed in the crystal by intermolecular hydrogen bonds.

Acknowledgements

We gratefully acknowledge the financial support from the Ministry of Higher Education, Science and Technology of the Republic of Slovenia for the financial support. We also thank EN-FIST Centre of Excellence (Ljubljana, Slovenia) for using SuperNova diffractometer.

Supplementary material

Structural and other crystallographic data for compounds **1** and **2** have been deposited with the Cambridge

Crystallographic Data Centre as supplementary publication numbers CCDC 936349 and 936350. A copy of the data can be obtained, free of charge, by applying to CCDC, 12 Union Road, Cambridge, CB2 1EZ, UK (fax: +44(0)-1223-336033 or e-mail: deposit@ccdc.cam.ac.uk).

References

[1] J. Kido, Y. Okamoto, Chem. Rev. 102, 2357 (2002)
[2] A. Gomez-Hens, M.P. Aguilar-Caballos, Trends. Anal. Chem. 21, 13 (2002)
[3] R.D. Rajasekhar, R. Laura, E. Pedro, M. Lawrence, Bioconjugate Chem. 22, 1402 (2011)
[4] J. Hongfei, W. Guilan, Z. Wenzhu, L. Xiaoyu, Y. Zhiqiang, J. Dayong, Y. Jingli, L. Zhiguang, J. Fluoresc. 20, 321 (2010)
[5] S. Faulkner, S.J.A. Pope, B.P. Burton-Pye, Appl. Spectrosc. Rev. 40, 1 (2005)
[6] J.W. Moore, M.D. Glick, W.A. Baker Jr., Am. Chem. J. 94, 6 (1971)
[7] G. Jia, G.L. Law, K.L. Wong, P.A. Tanner, W.T. Wong, Inorg. Chem. 47, 9431 (2008)
[8] L. Shuangxi, J. Linpei, Nat. Sci. 32, 96 (1996)
[9] B. Yan, Y. Bai, Z. Chen, J. Mol. Struct. 741, 141 (2005)
[10] W.T. Chen, Acta. Chim. Slov. 58, 144 (2011)
[11] Q. Yang, J.P. Zhao, B.W. Hu, X.F. Zhang, X.H. Bu, Inorg. Chem. 49, 3746 (2010)
[12] M.E. Chapman, P. Ayyappan, B.M. Foxman, G.T. Yee, W. Lin, Cryst. Growth. Des. 1, 159 (2001)
[13] Q.H. Jin, X. Li, Y.Q. Zou, K.B. Yu, Z. Kristallogr. 218, 45 (2003)
[14] K. Binnemans, Rare earths β-diketonates in Handbook on the Physics and Chemistry of Rare Earths (Elsevier, Amsterdam, 2005)
[15] N. Filipescu, W.F. Sager, F.A. Serafin, J. Phys. Chem. 68, 3324 (1964)
[16] W. Chen, S. Fukuzumi, Inorg. Chem. 48, 3800 (2009)
[17] L. Shen, M. Shi, F. Li, D. Zhang, X. Li, E. Shi, T. Yi, Y. Du, C. Huang, Inorg. Chem. 45, 6188 (2006)
[18] CrysAlis PRO. Version 1.171.35.11 (Agilent Technologies, Yarnton, Oxfordshire, England, 2011)
[19] A. Altomare, M.C. Burla, M. Camalli, G. Cascarano, C. Giacovazzo, A. Guagliardi, A.G.G. Moliterni, G. Polidori, R. Spagna, J. Appl. Cryst. 32, 115 (1999)
[20] G.M. Sheldrick, Acta. Cryst. A. 64, 112 (2008)
[21] L.J. Farrugia, J. Appl. Cryst. 30, 565 (1997)
[22] C.F. Macrae, P.R. Edgington, P. McCabe, E. Pidcock, G.P. Shields, R. Taylor, M. Towler, J. van de Streek, J. Appl. Cryst. 39, 453 (2006)
[23] R.D. Shannon, Acta. Cryst. A. 32, 751 (1976)
[24] H.W. Gu, S.X. Xiao, H.Y. Xiao, H.Y. Xiao, Y. Xiao, A.T. Li, X.L. Hu, Q.G. Li, Ind. Eng. Chem. Res. 51, 4797 (2012)
[25] P. Koczoń, J.Cz. Dobrowolski, W. Lewandowski, A.P. Mazurek, J. Mol. Struct. 655, 89 (2003)
[26] V.L. Dorofeev, Pharm. Chem. J. 38, 12 (2004)
[27] O. Khan, Molecular Magnets (VCH Publishers Inc., New York, 1993)